ACS Medicinal Chemistry Letters
Cite This: ACS Med. Chem. Lett. 2018, 9, 1099−1104
Letter
pubs.acs.org/acsmedchemlett

2-Aminoadipic Acid−C(O)−Glutamate Based Prostate-Specific Membrane Antigen Ligands for Potential Use as Theranostics

Ryo Nakajima,[†,⊥] Zora Nováková,[‡,⊥] Werner Tueckmantel,[§] Lucia Motlová,[‡] Cyril Bařinka,*[,‡] and Alan P. Kozikowski*[,§]

[†]Department of Medicinal Chemistry and Pharmacognosy, University of Illinois at Chicago, Chicago, Illinois 60612, United States
[‡]Institute of Biotechnology of the Czech Academy of Sciences, BIOCEV, Prumyslova 595, 252 50 Vestec, Czech Republic
[§]StarWise Therapeutics LLC, 505 South Rosa Road, Suite 27, Madison, Wisconsin 53719-1235, United States

Supporting Information

ABSTRACT: The design and synthesis of prostate specific membrane antigen (PSMA) ligands derived from 2-aminoadipic acid, a building block that has not previously been used to construct PSMA ligands, are reported. The effects of both the linker length and of an N-substituent of our PSMA ligands were probed, and X-ray structures of five of these ligands bound to PSMA were obtained. Among the ligands disclosed herein, **13b** showed the highest inhibitory activity for PSMA. As ligand **13b** can readily be radiolabeled since its fluorine atom is adjacent to the nitrogen atom of its pyridine ring, the use of this and related compounds as theranostics can be pursued.

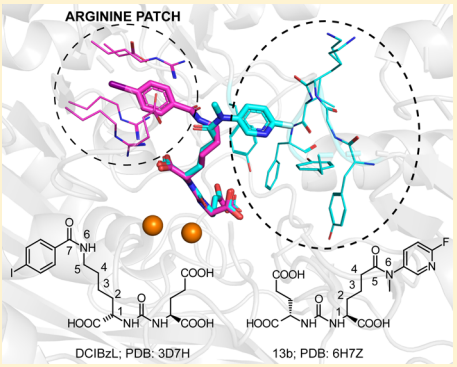

KEYWORDS: *Theranostic, PSMA ligands, prostate cancer, PET imaging, X-ray structure, arginine patch*

Prostate cancer (PCa) is the most frequently diagnosed cancer and the second leading cause of death in men in the US after lung cancer, with an estimated 180,890 new cases and 26,120 deaths in 2016. The aggregate cost of treating PCa patients has been estimated at $8−10 billion/year in the US, thus making it a significant disease with a heavy societal cost-burden.[1,2] The tissue-specific protein, prostate specific membrane antigen (PSMA), is an excellent target for imaging and therapy because it is a cell surface protein that presents a large extracellular target. Most PCa cells overexpress PSMA compared to the limited expression pattern observed in normal prostate cells, and the overexpression is significantly correlated to poor disease prognosis.[3−7] Therefore, several PSMA ligands including antibodies,[8,9] peptides,[10,11] aptamers,[12] and small molecules[13,14] have been developed to deliver imaging agents for the diagnosis of prostate cancer. Among them, small molecules exhibit favorable features: reproducible chemical synthesis, nonimmunogenicity, and, in general, fast clearance from normal tissues. In 2001, Kozikowski et al. first developed urea-based PSMA inhibitors as GCPII (glutamate carboxypeptidase II) inhibitors.[15] Since then, many researchers have been using this urea-based scaffold for targeting PSMA due to the high affinity of these ureas for PSMA as well as their ease of synthesis. Recently, these urea-based PSMA ligands labeled with ^{18}F or ^{68}Ga have been investigated as PET imaging agents in Phase III clinical trials.[16,17] However, such studies have revealed that uptake of these radioligands also takes place in off-target tissues including the kidneys and salivary glands, which might perhaps be avoided through proper design features. It is possible, for example, that such drawbacks can be overcome by enhancing the compounds' hydrophilicity, resulting in faster clearance from off-target tissues.[18,19] Even though hundreds of PSMA ligands have been explored in the past decades, the influence on PSMA affinity of the length of the second amino acid moiety (in addition to the obligatory P1′ glutamate) has not been elucidated yet since almost all of the PSMA ligands for PET imaging were synthesized starting from lysine or another molecule of glutamic acid.[16]

The internal substrate/inhibitor-binding cavity of PSMA can be divided into the prime (S1′) and nonprime sections separated by the active site harboring two Zn^{2+} ions (Figure 1A). Within the nonprime section, one of the most prominent structural features is the so-called arginine patch comprising Arg463, Arg534, and Arg536. Ionic interactions between the positively charged patch and the P1 carboxylate of PSMA-selective inhibitors are critical for the design of high affinity urea inhibitors. Furthermore, the flexibility of the arginine side chains allows for the formation of an S1 accessory hydrophobic pocket upon inhibitor binding that can be in turn exploited for the design of high affinity inhibitors as reported herein.[20−22] Our efforts focused on using 2-aminoadipic acid as a novel building block and to investigate the best chain length for

Received: July 15, 2018
Accepted: October 24, 2018
Published: October 24, 2018

DOI: 10.1021/acsmedchemlett.8b00318
ACS Med. Chem. Lett. 2018, 9, 1099−1104

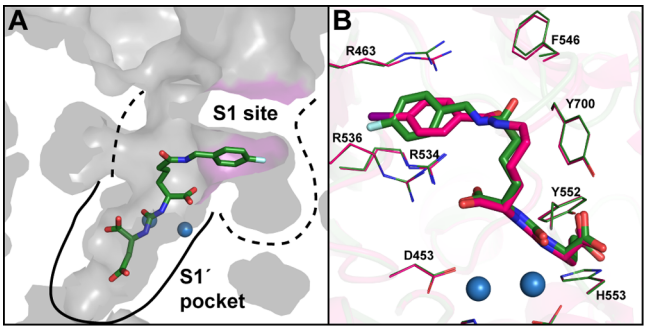

Figure 1. (A) Schematic representation of the internal cavity of PSMA (arginine patch, purple; zinc ions, light blue) in complex with **7a** (green sticks). (B) Comparison of the binding modes of **7a** (green) and **16** (DCIBzL, pink).

interaction with the S1 hydrophobic pocket to enhance the compounds' affinity for PSMA, with the goal of possibly reducing their dose of administration and achieving a higher image resolution.

We have chosen to concentrate on fluorinated PSMA ligands since it is well-known that the radionuclide ^{18}F has yielded improved imaging resolution compared to ^{68}Ga.[23] Fluorinated PSMA ligands incorporating 2-aminoadipic acid were synthesized as shown in Scheme 1. First, the distal carboxyl group of L-2-aminoadipic acid (enantiopurity: 98%) was protected by benzylation, and the monobenzyl ester was directly coupled with the enantiopure requisite isocyanate.[24] The free carboxyl group of **4** was protected as *tert*-butyl ester, and then the benzyl ester was deprotected by hydrogenation to form the carboxylic acid **6**. The desired amides **7**−**15** were obtained by amidation of **6**, followed by deprotection of the tri-*tert*-butyl esters. All final compounds **7**−**15** were purified by preparative high-performance liquid chromatography (preparative HPLC), and their chemical structures were confirmed by NMR and LCMS-IT-TOF. The purities of all tested compounds were >95%, as determined by analytical HPLC. The inhibition constants (IC_{50} values) of these compounds for the enzyme PSMA were determined using the radioenzymatic assay with [^{3}H]NAAG as a substrate (Table 1). The IC_{50} values of the

Scheme 1. Synthesis of Compounds 7−15[a]

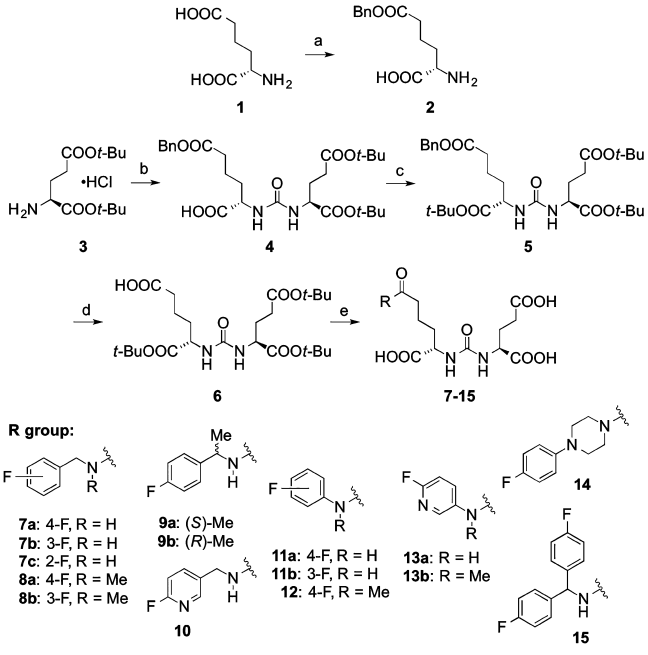

[a]Reagents and conditions: (a) 12 M HCl, BnOH, 100 °C, 1 h, 84%; (b) i. triphosgene, DIPEA, DCM, −78 °C, 1 h, then rt, 15 min; ii. **2**, DMF, −78 °C to r.t., overnight, 56%; (c) 2-*tert*-butyl-1,3-diisopropylisourea, DCM, reflux, overnight, 71%; (d) H_2, 10% Pd/C, MeOH, r.t., overnight, 80%; (e) i. amine, HATU, DIPEA, DMF, r.t., 16 h; ii. TFA, rt, 30 min. Yields: **7a**, 76%; **7b**, 89%; **7c**, 76%; **8a**, 89%; **8b**, 85%; **9a**, 72%; **9b**, 83%; **10**, 83%; **11a**, 79%; **11b**, 77%; **12**, 72%; **13a**, 62%; **13b**, 24%; **14**, 93%; **15**, 68%.

Table 1. PSMA Inhibitory Activity of Compounds 7a−c, 8a−b, 9a−b, 10, 9a−b, 12, 13a−b, 14, 15, 21a−b, and 22a−b[a]

compd	IC_{50} (nM)	compd	IC_{50} (nM)
7a	2.32 ± 0.55	**12**	0.20 ± 0.11
7b	2.91 ± 0.33	**13a**	0.99 ± 0.05
7c	2.11 ± 1.01	**13b**	0.075 ± 0.005
8a	0.64 ± 0.07	**14**	1.31 ± 0.18
8b	0.46 ± 0.10	**15**	1.19 ± 0.73
9a	5.24 ± 1.45	**21a**	0.94 ± 0.26
9b	5.44 ± 2.54	**21b**	0.15 ± 0.02
10	4.46 ± 1.03	**22a**	1.11 ± 0.22
11a	0.35 ± 0.01	**22b**	0.13 ± 0.01
11b	0.28 ± 0.09	**16** (DCIBzL)	0.021 ± 0.004

[a]Inhibition constants of studied compounds were determined using the radioenzymatic assay with [^{3}H]NAAG (radiolabeled at the terminal glutamate) as described previously.[22]

benzylamide derivatives **7a**−**7c** were almost identical, demonstrating that the position of the fluorine atom does not influence their potency. Introduction of a methyl group on the amide nitrogen of **7a** and **7b**, however, increased their potency for PSMA (compounds **8a** and **8b**). At the same time, however, compounds **9a** and **9b** that have a methyl group attached to the benzylic position showed approximately 2- and 10-fold lower inhibitory affinity for PSMA compared to **7a** and **8a**, respectively. The decrease in the inhibitory affinity of **9a** and **9b** is likely due to the steric hindrance of the methyl group clashing with the side chain of Arg463 and interfering thus with the full insertion of the inhibitor ring into the S1 hydrophobic accessory pocket. Additionally, it is plausible that the presence of the methyl group would also elicit a steric strain with the ring moiety within the inhibitor backbone at the rotation angle observed in the crystal structure of the PSMA/**7a** complex (see below). Compound **10**, in which the benzene ring is replaced with a pyridine ring, showed marginally lower affinity compared to **7a**.

To visualize the binding mode of one of our new PSMA ligands within the internal PSMA pocket, we first determined the crystal structure of the PSMA/**7a** complex to a final resolution of 1.48 Å (PDB code 5OF0). As expected, the position and interaction pattern of the urea-glutamate moiety in the S1′ pocket is identical to PSMA/urea-based inhibitor complexes published previously.[20] Favorably, and in-line with our hypothesis, the aromatic ring of **7a** is inserted into the S1 hydrophobic pocket, thereby increasing its inhibitor potency for PSMA through interactions contributed by the distal aromatic ring. It should be noted that the placement of the aromatic ring of **7a** is virtually identical to that observed in the complex of PSMA with DCIBzL, a urea-based inhibitor bearing

DOI: 10.1021/acsmedchemlett.8b00318
ACS Med. Chem. Lett. 2018, 9, 1099−1104

lysine as the main moiety of the P1 linkers (Figure 1B). These findings suggest that when there are seven intervening atoms between the urea function and the P1 aromatic moiety, the distal aromatic ring is preferably inserted into the hydrophobic accessory pocket within the arginine patch.

We next evaluated a series of compounds **11**−**13** having the P1 linker shortened by one atom, i.e., having six intervening atoms between the urea function and the P1 aromatic moiety, as this linker length has not been explored before. All compounds from this series showed subnanomolar IC_{50} values (Table 1) revealing that aminoadipic as the main moiety of the linker serves as an excellent substitute for the traditional lysine used in "canonical" urea-based compounds.

The affinities of the anilides **11**−**13** were on average higher than those of the corresponding benzylamides **7**−**10**, which indicates that the distance between the aromatic ring and the urea moiety in the former is more suitable for strong interactions with residues in the internal pocket of PSMA, an aspect of these urea-based ligands that was not explored in detail in previous studies.[24−27] Furthermore, the *N*-methylated anilides **12** and **13b** exhibited enhanced affinity compared with the corresponding *N*-H derivatives **11a** and **13a**, respectively. Particularly, **13b** showed the highest inhibitory activity (IC_{50} = 0.075 nM) for PSMA among all of the PSMA ligands synthesized from 2-aminoadipic acid.

To provide a mechanistic explanation for these SAR findings, we determined the crystal structures of **11a** (PDB code 6H7Y), **13a** (PDB code 6HKJ), and **13b** (PDB code 6H7Z) in complex with PSMA at a final resolution of 1.81, 2.09, and 2.00 Å, respectively (Supplementary Table S1). Compared to the structure of PSMA in complex with **7a**, which has the P1 aromatic ring inserted into the S1 hydrophobic pocket of the arginine patch, the position of the P1 aromatic moiety of both **11a** and **13a** differs substantially (Figure 2). For **11a** and **13a** the distal ring is inserted into a shallow pocket lined with the side chain of Y700 and the backbone of G206, K207, and V208. Also critical are F546, S547, G548, and W541, residues present within the flexible entrance lid[28] that form the opposite wall of the binding pocket (Figure S1).

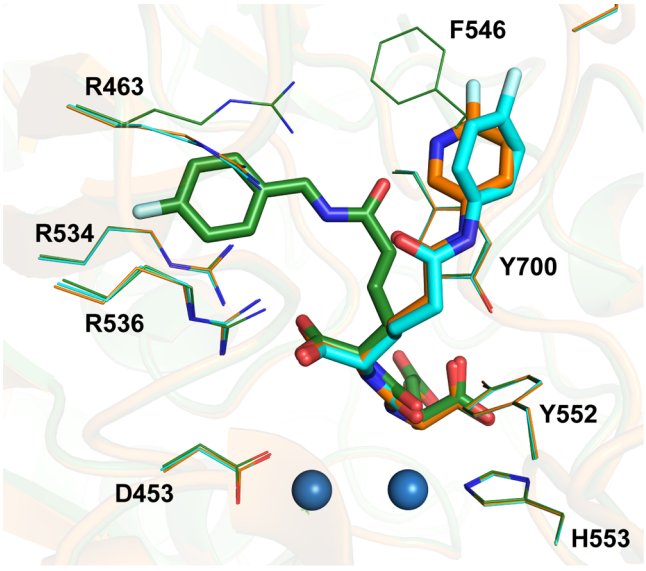

Figure 2. Comparison of binding modes of **7a** (green), **11a** (cyan), and **13a** (orange); zinc ions are shown as blue spheres. Note that while the positioning of the glutamate-urea moiety in the PSMA internal cavity is indistinguishable for both complexes, the distal aromatic rings occupy different portions of the entrance funnel due to differences in the length of the linker connecting the urea nitrogen and the distal aromatic ring (6 vs 7 intervening atoms).

Introduction of a *N*-methyl group into **13a**, leading to **13b**, is linked to a 10-fold increase in potency for PSMA and a slightly different interaction pattern. While the distal rings of **13b** and **13a** partially overlap, the former is inserted deeper into the pocket because of the cis conformation of the linking amide bond. Additionally, the increased potency of compounds with the pyridine ring in the cis conformation (e.g., **13b**) vs ones with either the phenyl group (e.g., **22b**) or pyridines in the trans conformation (e.g., **13a**) can likely be attributed to the water-mediated contact between the ring nitrogen and the hydroxyl group of Y234 (Figure S2). It should be noted that the above-mentioned hydrophobic patch is one of the interaction hotspots in the PSMA internal pocket as it is exploited by other inhibitory scaffolds such as hydroxamates or phosphoramidates.[21]

The data presented here together with prior studies[20,29] offer a comprehensive picture of relation between the P1 linker length and the position of the terminal aromatic moiety of urea-based compounds (Figure 3). For flexible linkers with

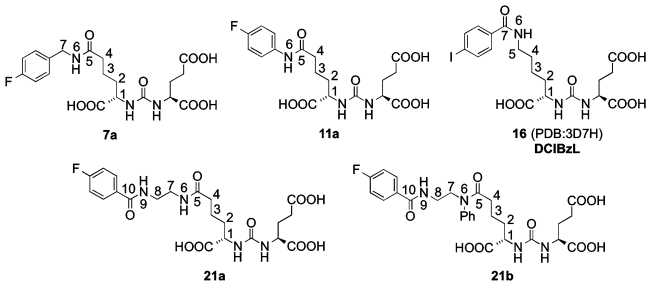

Figure 3. Chain length from the "left" nitrogen of the urea moiety to the aromatic ring in compounds **7a**, **11a**, **16**, **21a**, and **21b**.

seven intervening atoms, the distal aromatic ring will most likely be located within the S1 accessory pocket of the arginine patch. In the case of shorter (6 intervening atoms) and longer (>8 atoms) linkers the distal aromatic groups will either interact with one of the defined hydrophobic patches lining the entrance funnel or adopt several diverse conformations inside the funnel. It should be noted that a key aspect of the linker chain is its extreme flexibility. When comparing the structures of **7a** (reported here) and **16** (DCIBzL; PDB code 3D7H)[20] bound to PSMA, the position of their terminal halogenated rings inside the pocket is virtually identical, and this particular placement is facilitated by the linker's flexibility, as it can adopt several (most favorable) conformations within the spacious internal cavity.

The crystal structure of the PSMA/**13b** complex shows that the fluorinated pyridine ring of **13b** is constrained to adopt the *cis*-amide conformation with the *N*-methyl group pointing toward the unoccupied space of the entrance funnel (Figure 4A). This particular structural arrangement brings about the possibility of the addition of a second, larger substituent on the amide nitrogen. Such "branching" can be exploited for fine-tuning of both physicochemical and pharmacokinetic parameters to create the next generation of refined analogs.

To test this assumption, we synthesized compounds **21a,b** and **22a,b** as shown in Scheme 2. The starting material **18a**

DOI: 10.1021/acsmedchemlett.8b00318
ACS Med. Chem. Lett. 2018, 9, 1099−1104

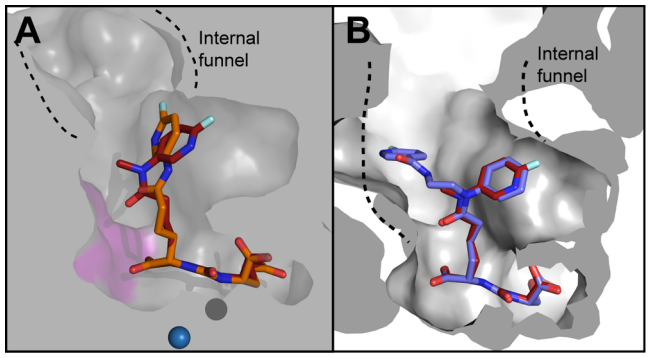

Figure 4. (A) Superposition of binding modes of **13a** (orange) and **13b** (red). (B) Detail of the amide methyl group (**13b**; red) and pyridine group (**22b**; blue; PDB code 6HKZ) pointing toward the unoccupied space of the internal funnel (dashed line).

Scheme 2. Synthesis of Compounds 21a–b and 22a–b[a]

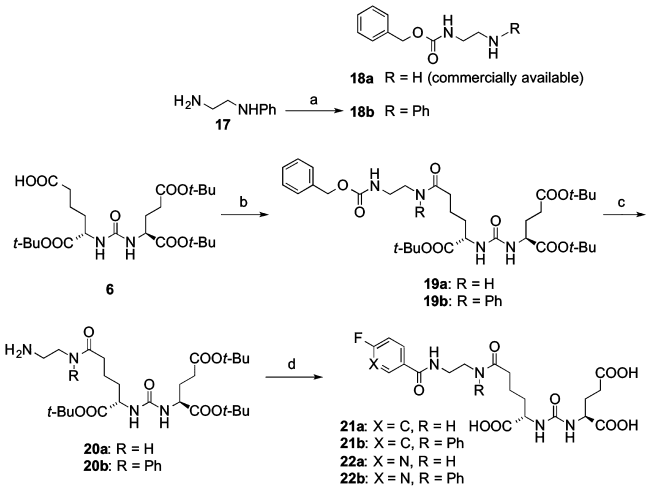

[a]Reagents and conditions: (a) Cbz-Cl, DIPEA, DCM, 0 °C to r.t., 1 h, 93%; (b) **18a** or **18b**, HATU, DIPEA, DMF, r.t., 16 h; (c) H_2, 10% Pd/C, MeOH, r.t., overnight. Yields: **20a**, 81%; **20b**, 59%; (d) i. carboxylic acid, HATU, DIPEA, DMF, r.t., 16 h; ii. TFA, r.t., 30 min. Yields: **21a**, 34%; **21b**, 52%; **22a**, 34%; **22b**, 57%.

was commercially available, while **18b** was obtained from *N*-phenyl-1,2-ethanediamine by monoprotection with a Cbz group. Both compounds underwent HATU-mediated amide formation with the building block **6** to give the *N*-H and *N*-Ph amide derivatives, respectively. The Cbz groups were removed by hydrogenation, and the obtained amines were reacted with 4-fluorobenzoic acid or 6-fluoronicotinic acid, followed by deprotection of the tri-*tert*-butyl esters to obtain the desired PSMA ligands **21a,b** and **22a,b**. As shown in Table 1, the derivatives **21b** and **22b** with an *N*-phenyl group exhibited 6- and 8-fold higher inhibitory activity for PSMA compared to the secondary amides **21a** and **22a**, respectively, suggesting that our strategy of using the phenyl ring as an anchor for these ligands is consistent with our working hypothesis (Figure 4B).

A similar strategy of using the distal P1 phenyl group as an anchor has been recently reported by Tykvart et al. However, exploiting the S1 accessory pocket of the arginine patch as an anchor point in their case led to mixed results as the insertion of the phenyl group into the pocket was unpredictable and strongly dependent on the physicochemical parameters of the branching functionality.[29] To the contrary, we believe that the structure-assisted branching strategy outlined in this Letter will be mostly independent of the nature of the branching functionality as it exploits the unoccupied space of the entrance funnel free of obvious steric barriers.

In conclusion, we have designed and synthesized PSMA ligands derived from 2-aminoadipic acid, a building block that has not previously been used to construct PSMA ligands. The effects of both the linker length and an N-substituent on our PSMA ligands were probed. Among these ligands, **13b** showed the highest inhibitory activity for PSMA. Moreover, the labeling methods previously described for [^{18}F]DCFPyL and [^{18}F]PSMA-1007[30,31] offer strong support that the preparation of [^{18}F]**13b** could be possible. Finally, a branching moiety can be attached to the amide function of **13b**, thus allowing the facile modulation of physicochemical and pharmacokinetic properties of the next generation of compounds while preserving the high affinity of the original compound for PSMA.

■ ASSOCIATED CONTENT

Supporting Information

The Supporting Information is available free of charge on the ACS Publications website at DOI: 10.1021/acsmedchemlett.8b00318.

Synthetic methods, analytical characterization of compounds, methods of crystallization, diffraction data collection and structure determination, data collection and refinement statistics, and enzymatic assays (PDF)

■ AUTHOR INFORMATION

Corresponding Authors

*(A.P.K.) E-mail: akozikowski@starwisetrx.com. Phone: (+1) 773-793-5866.

*(C.B.) E-mail: cyril.barinka@ibt.cas.cz. Phone: (+420) 325-873-777.

ORCID

Zora Nováková: 0000-0001-9804-6346

Cyril Bařinka: 0000-0003-2751-3060

Alan P. Kozikowski: 0000-0003-4795-5368

Author Contributions

⊥R.N. and Z.N. contributed equally.

Funding

We acknowledge Helmholtz–Zentrum Berlin for the allocation of synchrotron radiation beam time at the MX14.2 beamline and funding from the CALIPSOplus under the Grant Agreement 730872 from the EU Framework Programme for Research and Innovation HORIZON 2020. Additionally, this work was in part supported by the CAS (RVO: 86652036), MEYS CR (LM2015043 CIISB), and projects CIISB4-HEALTH (CZ.02.1.01/0.0/0.0/16_013/0001776) and BIO-CEV (CZ.1.05/1.1.00/02.0109) from the ERDF.

Notes

The authors declare no competing financial interest.

■ ACKNOWLEDGMENTS

The authors gratefully acknowledge I. Jelinkova and B. Havlinova for excellent technical assistance.

■ ABBREVIATIONS

SAR, structure–activity relationship; ZBG, zinc-binding group; DIPEA, *N*,*N*-diisopropylethylamine; DCM, dichloromethane;

DOI: 10.1021/acsmedchemlett.8b00318
ACS Med. Chem. Lett. 2018, 9, 1099–1104

HATU, 1-[bis(dimethylamino)methylene]-1*H*-1,2,3-triazolo-[4,5-*b*]pyridinium 3-oxide hexafluorophosphate; TFA, trifluoroacetic acid; PDB, Protein Data Bank

REFERENCES

(1) Siegel, R. L.; Miller, K. D.; Jemal, A. Cancer Statistics, 2016. *CA-Cancer J. Clin.* **2016**, *66* (1), 7−30.

(2) Wilson, L. S.; Tesoro, R.; Elkin, E. P.; Sadetsky, N.; Broering, J. M.; Latini, D. M.; DuChane, J.; Mody, R. R.; Carroll, P. R. Cumulative Cost Pattern Comparison of Prostate Cancer Treatments. *Cancer* **2007**, *109* (3), 518−527.

(3) O'Keefe, D. S.; Bacich, D. J.; Heston, W. D. Comparative Analysis of Prostate-Specific Membrane Antigen (PSMA) Versus a Prostate-Specific Membrane Antigen-Like Gene. *Prostate* **2004**, *58* (2), 200−210.

(4) Wang, X.; Yin, L.; Rao, P.; Stein, R.; Harsch, K. M.; Lee, Z.; Heston, W. D. Targeted Treatment of Prostate Cancer. *J. Cell. Biochem.* **2007**, *102* (3), 571−579.

(5) Ross, J. S.; Sheehan, C. E.; Fisher, H. A.; Kaufman, R. P., Jr.; Kaur, P.; Gray, K.; Webb, I.; Gray, G. S.; Mosher, R.; Kallakury, B. V. Correlation of Primary Tumor Prostate-Specific Membrane Antigen Expression with Disease Recurrence in Prostate Cancer. *Clin. Cancer Res.* **2003**, *9* (17), 6357−6362.

(6) Ghosh, A.; Heston, W. D. Tumor Target Prostate Specific Membrane Antigen (PSMA) and its Regulation in Prostate Cancer. *J. Cell. Biochem.* **2004**, *91* (3), 528−539.

(7) Mhawech-Fauceglia, P.; Zhang, S.; Terracciano, L.; Sauter, G.; Chadhuri, A.; Herrmann, F. R.; Penetrante, R. Prostate-Specific Membrane Antigen (PSMA) Protein Expression in Normal and Neoplastic Tissues and Its Sensitivity and Specificity in Prostate Adenocarcinoma: an Immunohistochemical Study Using Mutiple Tumour Tissue Microarray Technique. *Histopathology* **2007**, *50* (4), 472−483.

(8) Elsasser-Beile, U.; Reischl, G.; Wiehr, S.; Buhler, P.; Wolf, P.; Alt, K.; Shively, J.; Judenhofer, M. S.; Machulla, H. J.; Pichler, B. J. PET Imaging of Prostate Cancer Xenografts with a Highly Specific Antibody against the Prostate-Specific Membrane Antigen. *J. Nucl. Med.* **2009**, *50* (4), 606−611.

(9) Henry, M. D.; Wen, S.; Silva, M. D.; Chandra, S.; Milton, M.; Worland, P. J. A Prostate-Specific Membrane Antigen-Targeted Monoclonal Antibody−Chemotherapeutic Conjugate Designed for the Treatment of Prostate Cancer. *Cancer Res.* **2004**, *64* (21), 7995−8001.

(10) Aggarwal, S.; Singh, P.; Topaloglu, O.; Isaacs, J. T.; Denmeade, S. R. A Dimeric Peptide That Binds Selectively to Prostate-Specific Membrane Antigen and Inhibits Its Enzymatic Activity. *Cancer Res.* **2006**, *66* (18), 9171−9177.

(11) Rege, K.; Patel, S. J.; Megeed, Z.; Yarmush, M. L. Amphipathic Peptide-Based Fusion Peptides and Immunoconjugates for the Targeted Ablation of Prostate Cancer Cells. *Cancer Res.* **2007**, *67* (13), 6368−6375.

(12) Ni, X.; Zhang, Y.; Ribas, J.; Chowdhury, W. H.; Castanares, M.; Zhang, Z.; Laiho, M.; DeWeese, T. L.; Lupold, S. E. Prostate-Targeted Radiosensitization via Aptamer-shRNA Chimeras in Human Tumor Xenografts. *J. Clin. Invest.* **2011**, *121* (6), 2383−2390.

(13) Chen, Y.; Foss, C. A.; Byun, Y.; Nimmagadda, S.; Pullambahatla, M.; Fox, J. J.; Castanares, M.; Lupold, S. E.; Babich, J. W.; Mease, R. C.; Pomper, M. G. Radiohalogenated Prostate-Specific Membrane Antigen (PSMA)-Based Ureas as Imaging Agents for Prostate Cancer. *J. Med. Chem.* **2008**, *51* (24), 7933−7943.

(14) Barrett, J. A.; Coleman, R. E.; Goldsmith, S. J.; Vallabhajosula, S.; Petry, N. A.; Cho, S.; Armor, T.; Stubbs, J. B.; Maresca, K. P.; Stabin, M. G.; Joyal, J. L.; Eckelman, W. C.; Babich, J. W. First-in-Man Evaluation of 2 High-Affinity PSMA-Avid Small Molecules for Imaging Prostate Cancer. *J. Nucl. Med.* **2013**, *54* (3), 380−387.

(15) Kozikowski, A. P.; Nan, F.; Conti, P.; Zhang, J.; Ramadan, E.; Bzdega, T.; Wroblewska, B.; Neale, J. H.; Pshenichkin, S.; Wroblewski, J. T. Design of Remarkably Simple, Yet Potent Urea-Based Inhibitors of Glutamate Carboxypeptidase II (NAALADase). *J. Med. Chem.* **2001**, *44* (3), 298−301.

(16) Lutje, S.; Heskamp, S.; Cornelissen, A. S.; Poeppel, T. D.; van den Broek, S. A.; Rosenbaum-Krumme, S.; Bockisch, A.; Gotthardt, M.; Rijpkema, M.; Boerman, O. C. PSMA Ligands for Radionuclide Imaging and Therapy of Prostate Cancer: Clinical Status. *Theranostics* **2015**, *5* (12), 1388−1401.

(17) Rowe, S. P.; Gorin, M. A.; Allaf, M. E.; Pienta, K. J.; Tran, P. T.; Pomper, M. G.; Ross, A. E.; Cho, S. Y. PET Imaging of Prostate-Specific Membrane Antigen in Prostate Cancer: Current State of the Art and Future Challenges. *Prostate Cancer Prostatic Dis.* **2016**, *19* (3), 223−230.

(18) Chen, Y.; Lisok, A.; Chatterjee, S.; Wharram, B.; Pullambhatla, M.; Wang, Y.; Sgouros, G.; Mease, R. C.; Pomper, M. G. [18F]Fluoroethyl Triazole Substituted PSMA Inhibitor Exhibiting Rapid Normal Organ Clearance. *Bioconjugate Chem.* **2016**, *27* (7), 1655−1662.

(19) Huang, S. S.; Wang, X.; Zhang, Y.; Doke, A.; DiFilippo, F. P.; Heston, W. D. Improving the Biodistribution of PSMA-Targeting Tracers With a Highly Negatively Charged Linker. *Prostate* **2014**, *74* (7), 702−713.

(20) Barinka, C.; Byun, Y.; Dusich, C. L.; Banerjee, S. R.; Chen, Y.; Castanares, M.; Kozikowski, A. P.; Mease, R. C.; Pomper, M. G.; Lubkowski, J. Interactions between Human Glutamate Carboxypeptidase II and Urea-Based Inhibitors: Structural Characterization. *J. Med. Chem.* **2008**, *51* (24), 7737−7743.

(21) Novakova, Z.; Wozniak, K.; Jancarik, A.; Rais, R.; Wu, Y.; Pavlicek, J.; Ferraris, D.; Havlinova, B.; Ptacek, J.; Vavra, J.; Hin, N.; Rojas, C.; Majer, P.; Slusher, B. S.; Tsukamoto, T.; Barinka, C. Unprecedented Binding Mode of Hydroxamate-Based Inhibitors of Glutamate Carboxypeptidase II: Structural Characterization and Biological Activity. *J. Med. Chem.* **2016**, *59* (10), 4539−4550.

(22) Novakova, Z.; Cerny, J.; Choy, C. J.; Nedrow, J. R.; Choi, J. K.; Lubkowski, J.; Berkman, C. E.; Barinka, C. Design of Composite Inhibitors Targeting Glutamate Carboxypeptidase II: the Importance of Effector Functionalities. *FEBS J.* **2016**, *283* (1), 130−143.

(23) Sanchez-Crespo, A. Comparison of Gallium-68 and Fluorine-18 Imaging Characteristics in Positron Emission Tomography. *Appl. Radiat. Isot.* **2013**, *76*, 55−62.

(24) Wang, H.; Byun, Y.; Barinka, C.; Pullambhatla, M.; Hyo-eun, C. B.; Fox, J. J.; Lubkowski, J.; Mease, R. C.; Pomper, M. G. Bioisosterism of Urea-Based GCPII Inhibitors: Synthesis and Structure−Activity Relationship Studies. *Bioorg. Med. Chem. Lett.* **2010**, *20* (1), 392−397.

(25) Maresca, K. P.; Hillier, S. M.; Femia, F. J.; Keith, D.; Barone, C.; Joyal, J. L.; Zimmerman, C. N.; Kozikowski, A. P.; Barrett, J. A.; Eckelman, W. C.; Babich, J. W. A Series of Halogenated Heterodimeric Inhibitors of Prostate Specific Membrane Antigen (PSMA) as Radiolabeled Probes for Targeting Prostate Cancer. *J. Med. Chem.* **2008**, *52* (2), 347−357.

(26) Pavlicek, J.; Ptacek, J.; Cerny, J.; Byun, Y.; Skultetyova, L.; Pomper, M. G.; Lubkowski, J.; Barinka, C. Structural Characterization of P1'-Diversified Urea-Based Inhibitors of Glutamate Carboxypeptidase II. *Bioorg. Med. Chem. Lett.* **2014**, *24* (10), 2340−2345.

(27) Yang, X.; Mease, R. C.; Pullambhatla, M.; Lisok, A.; Chen, Y.; Foss, C. A.; Wang, Y.; Shallal, H.; Edelman, H.; Hoye, A. T.; Attardo, G.; Nimmagadda, S.; Pomper, M. G. [18F]-Fluorobenzoyllysinepentanedioic Acid Carbamates: New Scaffolds for Positron Emission Tomography (PET) Imaging of Prostate-Specific Membrane Antigen (PSMA). *J. Med. Chem.* **2016**, *59* (1), 206−218.

(28) Barinka, C.; Hlouchova, K.; Rovenska, M.; Majer, P.; Dauter, M.; Hin, N.; Ko, Y. S.; Tsukamoto, T.; Slusher, B. S.; Konvalinka, J.; Lubkowski, J. Structural Basis of Interactions between Human Glutamate Carboxypeptidase II and Its Substrate Analogs. *J. Mol. Biol.* **2008**, *376* (5), 1438−1450.

(29) Tykvart, J.; Schimer, J.; Jancarik, A.; Barinkova, J.; Navratil, V.; Starkova, J.; Sramkova, K.; Konvalinka, J.; Majer, P.; Sacha, P. Design of Highly Potent Urea-Based, Exosite-Binding Inhibitors Selective for

DOI: 10.1021/acsmedchemlett.8b00318
ACS Med. Chem. Lett. 2018, 9, 1099−1104

Glutamate Carboxypeptidase II. *J. Med. Chem.* **2015**, *58* (10), 4357−4363.
(30) Giesel, F. L.; Hadaschik, B.; Cardinale, J.; Radtke, J.; Vinsensia, M.; Lehnert, W.; Kesch, C.; Tolstov, Y.; Singer, S.; Grabe, N.; Duensing, S.; Schafer, M.; Neels, O. C.; Mier, W.; Haberkorn, U.; Kopka, K.; Kratochwil, C. F-18 Labelled PSMA-1007: Biodistribution, Radiation Dosimetry and Histopathological Validation of Tumor Lesions in Prostate Cancer Patients. *Eur. J. Nucl. Med. Mol. Imaging* **2017**, *44* (4), 678−688.
(31) Ravert, H. T.; Holt, D. P.; Chen, Y.; Mease, R. C.; Fan, H.; Pomper, M. G.; Dannals, R. F. An Improved Synthesis of the Radiolabeled Prostate-Specific Membrane Antigen Inhibitor, [(18) F]DCFPyL. *J. Labelled Compd. Radiopharm.* **2016**, *59* (11), 439−450.

NOTE ADDED AFTER ASAP PUBLICATION

This paper published ASAP on 10/30/2018 with an incorrect image for the TOC/Abstract. The image was replaced, and the revised version was reposted on 11/8/2018.

DOI: 10.1021/acsmedchemlett.8b00318
ACS Med. Chem. Lett. 2018, 9, 1099−1104